Heat Transfer in a Fuel Cell Battery

DIMITRI GIDASPOW and BERNARD S. BAKER

Institute of Gas Technology, Chicago, Illinois

Analytical solutions were obtained for temperature distributions in a single adiabatic fuel cell with heat generation by $T\Delta S$, I^2R, and polarization. With these results it is possible to characterize heat transfer in a battery with convection in the fuel and air streams, and with conduction of heat in three directions, by means of an average temperature for which an analytical solution was also obtained. Although the temperature can be kept within safe limits in low-power density batteries, the results show that critical dimensions exist beyond which failure by thermal buckling will occur.

Fuel cell technology has reached the stage where batteries of cells are being assembled into complete power plants. In most instances it is desirable to maintain fuel cell operation within a narrow temperature range. Since several heat generation and dissipation processes can exist in a fuel cell, a more complete heat transfer analysis is required than has been previously published (*3, 4*). This paper develops methods of predicting temperature profiles and design parameters in fuel cells with a stationary electrolyte where cooling takes place by convection and conduction. Two cases have been considered: a one-dimensional analysis of a single adiabatic fuel cell, and a three-dimensional analysis of a multicell battery.

A SINGLE FUEL CELL

This analysis shows how the electrolyte temperature of a single cell inside a battery can vary with length of cell when heat is generated reversibly by $T\Delta S$ dissipation, and irreversibly by resistance heating and polarization at the electrodes with no decrease in temperature due to conduction of heat. This simplified treatment will justify the use of an average temperature in analyzing heat transfer in a battery, and will indicate the limitations of such an analysis.

Material and energy balances formulated in this section of the paper refer to parallel flow of air and a fuel in essentially parallel plate channels of a fuel cell of a flow-through configuration, as shown in Figure 1. Lateral heat transfer from element to element or from the fuel cell element to the wall, and conduction of heat through the element perpendicular to the direction of mass flow, is neglected in the derivation of the energy balances. The situation considered thus represents the case of a thermally insulated fuel cell with energy transferred only by the gases and by the electric current produced.

Current Distribution

On the grounds that a quantitative study of a simple case provides valuable qualitative insight into a more complex one, the rate of reaction at the electrode surface is assumed to be of first order with respect to the controlling species, i. This assumption is expected to hold in many situations, as discussed by Levich (*6*) and by Austin, Palasi, and Klimpel (*1*). For the fuel cell situations in which the local current is a weaker function of concentration, the analysis in this section may be extended to fractional and zero-order rates. Here

$$\text{rate} = Ky_i,\ K = f(\Delta E) \qquad (1)$$

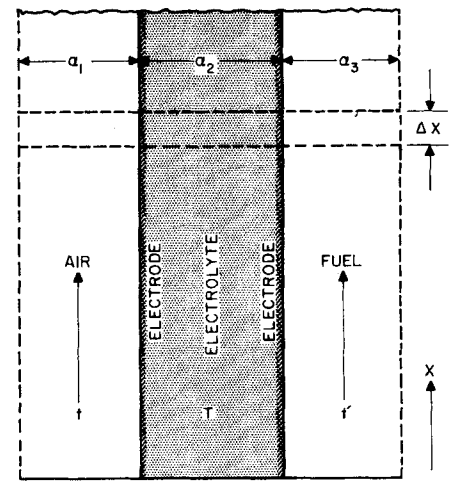

Fig. 1. Cross section of a fuel cell for material and energy balances.

The overall rate constant K will, in general, be a function of the electromotive potential difference in an operating fuel cell, and can be considered to be made up of contributions due to diffusion and to reaction at the surface, in the usual manner (*5*). For a gas channel diffusion-controlled process, K is the usual mass transfer coefficient multiplied by total pressure. It is also assumed that ΔE is not a function of concentration over the range of conversions encountered. Such an assumption is valid in at least some of the work discussed by Levich (*6*), and can be used here as a first approximation. It should also be observed that the use of current collectors with good electrical conductivity will cause the potential difference between the anode and the cathode to be constant over the length of the cell and therefore not a function of concentration. Thus for a given ΔE, the current or rate constant K can be considered as known for an experimentally determined function, f. Conservation of the controlling species in the air stream and the first-order reaction with back diffusion neglected yields

$$\alpha_1 \frac{d(Cvy_i)}{dx} = -Ky_i \qquad (2)$$

Neglecting the small change in the total number of moles in the air stream for incomplete conversion gives the local current density distribution

$$I = nFKy_i^{\circ} \exp\left(-\frac{Kx}{\alpha_1 Cv}\right) \tag{3}$$

Integration of the current over the electrode length L and division by L yields the average current density usually reported in fuel cell work.

$$I_{av} = nF \cdot \frac{\alpha_1}{L} \cdot (Cv) \cdot (y_i^{\circ} - y_i') \tag{4}$$

Equation (4) simply represents an overall species balance for the fuel cell.

Energy Balances

The electrolyte, the anode, and the cathode are assumed to be in sufficiently intimate contact and thin enough so that they are at the same temperature at any longitudinal position. In addition, for the thin, long elements, the heat transferred by conduction vs. that by convection can be neglected for the thermally insulated cell considered here. Also, for this parallel flow-through cell, heating or cooling due to sensible enthalpy differences of gaseous reactants and gaseous products entering and leaving the small element Δx in Figure 1 are negligible. Heat can be generated by three modes in the fuel cell element: $T\Delta S$ dissipation, ohmic dissipation, and polarization losses. For the range of current densities of interest the sum of polarizations at the anode and at the cathode, ΔE_p, can be represented to a good approximation by a straight line (7). Should this not be sufficiently accurate, the polarization can be fitted to a general polynomial of current density and the analysis repeated without mathematical difficulty. For this analysis

$$\Delta E_p = \beta_0 + \beta_1 I \tag{5}$$

The energy balance obtained by equating the net rate of energy outflow by convection to the fuel and air streams to the rate of energy dissipation by $T\Delta S$, ohmic, and polarization contributions yields

$$h(T-t) + h'(T-t') = I\left(3.413\,\beta_0 - \frac{T_m \Delta S}{nF}\right) + 3.413\,I^2\left(\beta_1 + \frac{\alpha_2}{\sigma}\right) \tag{6}$$

In Equation (6) the temperature T_m associated with $T_m\Delta S$ is the absolute temperature, while all other temperatures can be referred to some given initial temperature. Thus, temperatures not associated with entropy can be regarded as deviations from some base temperature. If these deviations or perturbations are not large compared with the absolute temperature, the absolute temperature in the $T_m\Delta S$ term and ΔS may be evaluated at some mean value; thus the generation terms may be regarded as independent of temperature.

The energy balance for the air phase, neglecting conduction and any sensible enthalpy differences due to mass addition or subtraction, becomes

$$\rho v \alpha_1 c_p \frac{dt}{dx} + h(t-T) = 0 \tag{7}$$

A similar balance must be written for the fuel stream with primed quantities referring to the fuel side.

These equations, together with the feed temperatures of the air stream t_o, and of the fuel stream t_o', completely determine the electrolyte, fuel, and air temperatures.

Electrolyte Temperature

In terms of the groups defined in the Notation section of this paper, it is possible to give a simple expression for the electrolyte temperature as a function of fuel cell length.

$$T = \frac{T_S}{1+m}\left[1 + \frac{H_h - H_m}{H_m}\exp\left(-\frac{x}{H_m}\right)\right] + \frac{T_R}{1+m}\left[1 + \frac{2H_h - H_m}{H_m}\exp\left(-\frac{2x}{H_m}\right)\right] + \frac{t_o + nt_o'}{1+n} + \frac{(n-m)(t_o - t_o')}{(1+n)(1+m)} \exp\left[-\frac{m(1+n)x}{n(1+m)H_h}\right] \tag{8}$$

The first two terms are contributions of heat generation by $T\Delta S$ *plus* polarization and by I^2R *plus* polarization losses, respectively. The last two terms result from unequal inlet temperatures, mass flows, and heat capacities of the two streams. Figure 2 shows the different behavior of the electrolyte temperature for different ratios of heights of heat transfer to mass transfer units.

Gas Temperatures

The air stream temperature is given by

$$t = \frac{T_s}{1+m}\left[1 - \exp\left(-\frac{x}{H_m}\right)\right] + \frac{T_R}{1+m}\left[1 - \exp\left(-\frac{2x}{H_m}\right)\right] + \frac{n(t_o - t_o')}{1+n}\exp\left[-\frac{m(1+n)x}{n(1+m)H_h}\right] + \frac{t_o + nt_o'}{1+n} \tag{9}$$

The fuel stream temperature is

$$t' = \frac{T_S}{1+m}\left[1 - \exp\left(-\frac{x}{H_m}\right)\right] + \frac{T_R}{1+m}\left[1 - \exp\left(-\frac{2x}{H_m}\right)\right] + \frac{t_o' - t_o}{1+n}\exp\left[-\frac{m(1+n)x}{n(1+m)H_h}\right] + \frac{t_o + nt_o'}{1+n} \tag{10}$$

All the temperatures—T, t, and t'—approach the same constant value as x increases without limit, as would be expected. For positive heat generation terms and equal inlet temperatures, the gas temperatures always increase with length, also as expected.

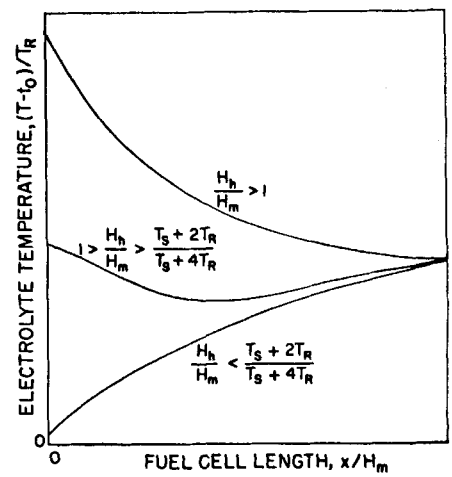

Fig. 2. Electrolyte temperature behavior at equal inlet air and fuel temperatures with no conduction.

Discussion

It is interesting to exhibit the behavior of the temperature in Equation (8). This is best done by removing the complication of possible unequal inlet air and fuel temperatures. For such a case a minimum temperature of the electrolyte occurs for positive T_S and T_R when the ratio of H_h to H_m lies between the limits shown in Figure 2. For slow reactions, that is, low current densities, H_h is much smaller than H_m and the temperature will rise with length. This is the usual and expected behavior. The electrolyte and the gases become hotter as more heat is generated. For rapid reactions it takes a smaller length, H_m, to achieve a unit of conversion than it does for slow reactions. Thus the ratio of H_h to H_m is larger. The effect of the rate of reaction decreasing with concentration becomes important, and the electrolyte temperature begins to drop. A monotonic decrease of electrolyte temperature with length is thus obtained at very high current densities.

Analysis of the difference between the electrolyte temperature and one of the gas temperatures, for example, the air temperature, is informative. For equal inlet air and fuel temperatures $(T - t)$ is as shown below.

$$(T-t) = \frac{1}{1+m} \cdot \frac{H_h}{H_m} \left\{ T_S e^{-\frac{x}{H_m}} + 2\,T_R e^{-\frac{2x}{H_m}} \right\} \tag{11}$$

Equation (11) shows that for very small ratios of H_h to H_m and only moderately high values of T_S and T_R, the electrolyte and the gas temperatures become equal. This equation also makes it clear that for low current densities the electrolyte temperature tends to rise with length, because the electrolyte temperature almost equals the gas temperature.

In order to relate the above equations to an actual experimental situation, the characteristics of the Institute of Gas Technology's low-temperature fuel cell were used. For this low-temperature fuel cell (70°C.) operating on reformed natural gas and air (with a 1/32-in. half-spacing in the air channel, an average current density of 40 ma./sq. cm., and a 10% oxygen in the air conversion in a 1-ft.-long cell) the H_m is 9.57 ft., H_h is 0.0392 ft., and T_S is about 380°F. T_R may be as much as several times the value of T_S, for example 1,000°F. These values, approximate as yet, show that it will be possible generally to assume equality of electrolyte and gas temperatures away from the entrance, because they will differ by only a few degrees. Because these deviations will also be relatively small for the high-temperature fuel cells, it will be possible to characterize three-dimensional heat transfer in such a fuel cell pack by the use of one average temperature, as is the common practice in packed beds. Neglect of conduction in this analysis gives only higher differences between the electrolyte and the gas temperatures, because heat loss from the ends of the cell reduces the electrolyte temperature. The case examined was therefore the worst possibility.

THREE-DIMENSIONAL ANALYSIS OF A BATTERY

The solution for the temperature distribution in a fuel cell pack in this section is based on the following assumptions:

1. The gas and the electrolyte temperatures are not very different from each other. Equation (11) shows that this will be true for small ratios of heat transfer to reaction units.

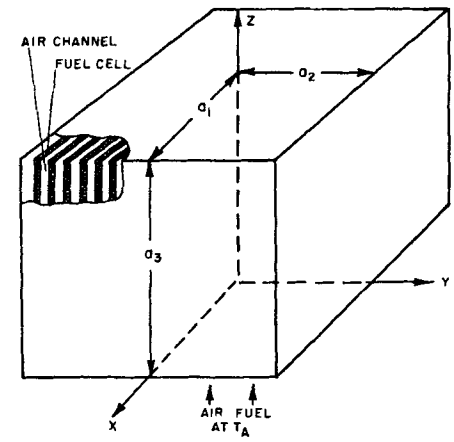

Fig. 3. Fuel cell pack.

2. The sensible heat differences between the fuel and the reaction products are either small due to low flow rates, or they can be included with the sensible heat changes of the air stream.

3. The rate of heat generation is constant per unit volume of pack. The source term is evaluated at an average pack temperature.

4. The process has reached a steady state.

The analysis refers to a rectangular fuel cell pack, $2a_1$ units wide, $2a_2$ units long, and a_3 units high. The cells in the pack have their faces perpendicular to the y axis, as shown in Figure 3. Air enters the channels at temperature T_A at the bottom and flows up in the air spaces. All the walls, excluding the bottom of the pack, will be maintained at a constant temperature, T_W. This appears to be a practical requirement to assure that the cells and portions of the cells near the faces of the pack remain at a sufficiently high temperature to stay operative. Sufficient insulation will be used to maintain the faces at T_W. These boundary conditions are believed to be more realistic than convection boundary conditions.

Energy Balance

The steady state energy balance at constant pressure yields

$$G\,c_p \frac{\partial T}{\partial z} + \frac{\partial q_x}{\partial x} + \frac{\partial q_y}{\partial y} + \frac{\partial q_z}{\partial z} = \psi \tag{12}$$

Further, let

$$q_x = -k_x \frac{\partial T}{\partial x},$$

where

$$k_x = k_{\text{metal and electrolyte}} \cdot \frac{A_{\text{metal and electrolyte}}}{A_{\text{total}}} \tag{13}$$

Similarly, define q_z and, due to symmetry, let k_x equal k_z and call both k. This effective thermal conductivity is obtained by adding the area fractions of the conductivities of the component parts of a fuel cell. Heat in the y direction will flow by conduction through the spacers separating the cells and by convection and radiation between the cells, as well as by conduction through the electrolyte-electrode combination. A reasonable way to handle such heat flow appears to be the use of an effective thermal conductivity, as is generally done in packed beds. This effective thermal conductivity, k_r, would have to be measured for a given configuration or estimated by summing all resistances. Assuming the thermal conductivities to be independent of temperature, the partial differential equation becomes

$$k\frac{\partial^2 T}{\partial x^2} + k_r\frac{\partial^2 T}{\partial y^2} + k\frac{\partial^2 T}{\partial z^2} - Gc_p\frac{\partial T}{\partial z} = -\psi \quad (14)$$

The boundary conditions (BC) are as follows:

$$\frac{\partial T\ (0, y, z)}{\partial x} = 0, \text{ by symmetry} \quad \text{(BC 1)}$$

$$T\ (a_1, y, z) = T_w \quad \text{(BC 2)}$$

$$\frac{\partial T\ (x, 0, z)}{\partial y} = 0, \text{ by symmetry} \quad \text{(BC 3)}$$

$$T\ (x, a_2, z) = T_w \quad \text{(BC 4)}$$

$$T\ (x, y, 0) = T_A, \quad \text{(BC 5)}$$

since the bottom face is near the entering air temperature

$$T\ (x, y, a_3) = T_w \quad \text{(BC 6)}$$

To write the partial differential equation in dimensionless form, an adiabatic reaction temperature, T_{ad}, is used as a scale factor for obtaining a reduced temperature. The coordinates are scaled down using the dimensions of the pack. Defining a Peclet number, N_{Pe}, and two other dimensionless parameters, b_1 and b_2, the conservation of energy equation can be written in dimensionless form.

$$b_1^2\frac{\partial^2 \bar{T}}{\partial \bar{x}^2} + b_2^2\frac{\partial^2 \bar{T}}{\partial \bar{y}^2} + \frac{\partial^2 \bar{T}}{\partial \bar{z}^2} - N_{Pe}\frac{\partial \bar{T}}{\partial \bar{z}} = -N_{Pe} \quad (15)$$

Expressed in dimensionless form, all boundary conditions except BC 5 become homogeneous. The dimensionless temperature at the boundary of BC 5 becomes $\bar{T}_A$.

Solution

Equation (15) with its six boundary conditions was solved by applying the principle of superposition several times. The differential equation was made homogeneous by subtracting from $\bar{T}$ the solution to the corresponding one-dimensional problem in the z direction. The resulting boundary value problem has two of its boundary conditions, BC 2 and BC 4, nonhomogeneous. This problem was solved by expressing the temperature function as the sum of one problem with BC 2 homogeneous *plus* the other with BC 4 homogeneous. Then the classical separation of variables method was used.

The temperature distribution in the pack is as follows:

$$\bar{T}\ (\bar{x}, \bar{y}, \bar{z}) = \bar{z} - Q - R\exp\ (N_{Pe}\bar{z}) + \sum_{n=1}^{\infty}\sum_{m=0}^{\infty} A_{nm}\exp\left(N_{Pe}\frac{\bar{z}}{2}\right)\sin n\pi\bar{z}\cos\left(\frac{2m+1}{2}\right)\pi\bar{x}\cosh p_{nm}\bar{y}$$

$$+\sum_{n=1}^{\infty}\sum_{m=0}^{\infty} B_{nm}\exp\left(N_{Pe}\frac{\bar{z}}{2}\right)\sin n\pi\bar{z}\cos\left(\frac{2m+1}{2}\right)\pi\bar{y}\cosh q_{nm}\bar{x} \quad (16)$$

where

$$A_{nm} = \frac{8N_{Pe}(-1)^m}{n\pi^2(2m+1)[\exp\ (N_{Pe}) - 1]\cosh p_{nm}}\left\{\left[Q + \frac{4N_{Pe}}{4n^2\pi^2 + N_{Pe}^2}\right]\cdot\left[1 - (-1)^n\exp\left(\frac{1}{2}N_{Pe}\right)\right]\right.$$

$$\left. + \left[\frac{R(4n^2\pi^2 + N_{Pe}^2)}{(4n^2\pi^2 + 9N_{Pe}^2)}\right]\cdot\left[1 - (-1)^n\exp\left(\frac{3}{2}N_{Pe}\right)\right] + (-1)^n\exp\left(\frac{1}{2}N_{Pe}\right)\right\} \quad (17)$$

$$B_{nm} = A_{nm}\frac{\cosh p_{nm}}{\cosh q_{nm}} \quad (18)$$

$$p_{nm} = \frac{1}{b_2}\left[\left(\frac{1}{2}N_{Pe}\right)^2 + n^2\pi^2 + \left(\frac{b_1}{2}\right)^2\pi^2(2m+1)^2\right]^{1/2} \quad (19)$$

$$q_{nm} = \frac{1}{b_1}\left[\left(\frac{1}{2}N_{Pe}\right)^2 + n^2\pi^2 + \left(\frac{b_2}{2}\right)^2\pi^2(2m+1)^2\right]^{1/2} \quad (20)$$

$$Q = \frac{1 + \bar{T}_A\exp\ (N_{Pe})}{1 - \exp\ (N_{Pe})} \quad (21)$$

$$R = \frac{1 + \bar{T}_A}{\exp\ (N_{Pe}) - 1} \quad (22)$$

The first three terms represent the solution to the one-dimensional problem in the z direction. They give the temperature distribution in the pack with its four sides insulated. The first of these three arises due to a constant rate of heat generation with no conduction, while the other two show the effect of longitudinal conduction. The two double series correct for the heat loss from the sides of the pack.

This solution does not appear to have been given previously in the literature (2).

Numerical

To obtain temperature distributions in a fuel cell battery for a given anticipated cell design, the dimension and thermal-conductivity-dependent parameters are first estimated. As an illustrative example, Institute of Gas Technology's reformed natural gas molten carbonate fuel cell, operating at about 500°C., will be used as the basis for discussion. For an effective cell thickness of about 0.4 in., the thermal conductivity in the direction of flow k was estimated to be 12.2 B.t.u./hr.-ft.-°F., while a value of 0.76 was obtained for k_r. Then, for a 1.5-ft. cubical battery, b_1 and b_2 are 2 and 0.5, respectively. To determine the adiabatic temperatures and Peclet numbers, the necessary flow rates were calculated as a function of current density from the species balance [Equation (4)] for a 20% conversion of oxygen in the air stream. Heat generation was obtained from experimental polarization data for various current densities. The resulting adiabatic temperature and Peclet numbers are shown in Figure 4 as a function of current density.

A Fortran program for summing the double infinite series in Equation (16) was written and temperature dis-

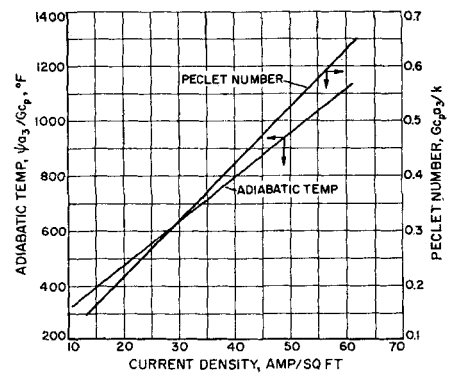

Fig. 4. Adiabatic temperature and Peclet number.

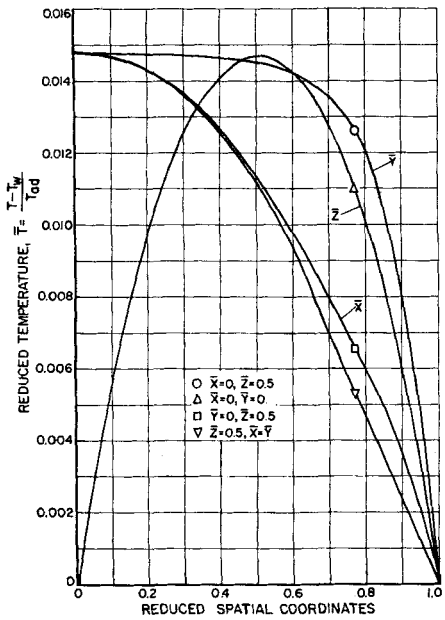

Fig. 5. Reduced temperature for a reduced inlet temperature of zero, Peclet number of 0.2, b_1 equal to 2.0, and b_2 equal to 0.5.

tributions for two inlet gas temperatures and three Peclet numbers obtained.

Figure 5 shows a monotonic decrease of temperature in the $\bar{x}$ and $\bar{y}$ directions, from the maximum at the center to zero at the faces, as expected from physical considerations. It appears that due to a lower thermal conductivity in the $\bar{y}$ direction, 0.76 B.t.u./hr.-ft.-°F. *vs.* 12.2 B.t.u./hr.-ft.-°F., the $\bar{y}$ profile at the center of the pack is at first quite flat. The temperature profile at the midpoint of the cell in direction of flow is also shown for the diagonal $\bar{x} = \bar{y}$. The temperature in the $\bar{z}$ direction goes through a maximum at the center of the cell. The maximum need not be at the exact center of the cell, but is indistinguishably close to it in this case, due to the small value of the Peclet number and the large lateral heat losses. The negative slopes of the temperature profiles show that there is heat loss at five faces. The positive slope of the $\bar{z}$ curve at the gas inlet face shows that heat must also be removed from this face to maintain it at zero-reduced temperature. Point heat fluxes at the walls of the battery can be obtained from the graphs by measuring the slopes of the temperature profiles. The maximum heat fluxes for the $\bar{y}$ and $\bar{x}$ faces obtained from Figure 5 are 40 and 245 B.t.u./hr.-sq. ft., respectively.

Figure 6 shows similar temperature profiles for a higher Peclet number. It may be noted that tripling the Peclet number, which is essentially tripling the current density, roughly triples the maximum dimensionless temperature. This causes a greater effect on the maximum absolute temperature of the pack, increasing it by over a factor of six. This is due to the increase caused in the adiabatic temperature by the increase in current density.

At the current density corresponding to this Peclet number—57 amp./sq. ft.—the highest temperature in the battery is about 50°F. above the wall temperature. This is close to the allowable limit for safe, prolonged operation. A serious heat transfer problem will arise in such batteries at higher power densities, lower effective conductivities, and bigger packs.

Figure 7 shows the effect of a higher inlet reduced temperature at an intermediate Peclet number. Here the temperature in the $\bar{z}$ direction monotonically decreases from the inlet on.

THERMAL BUCKLING IN A BATTERY

For the case of the rate of heat generation increasing rapidly with temperature, the rate of energy dissipation in the fuel cell pack is linearized locally as follows:

$$\psi = \psi_o + \psi_1 T \tag{23}$$

Heat generation can increase with temperature by virtue of a negative entropy change.

Using the same definitions of constant effective thermal conductivities, the unsteady state energy equation expressed in dimensionless form becomes

$$\frac{\partial \hat{T}}{\partial \theta} = \frac{\partial^2 \hat{T}}{\partial \bar{z}^2} - N_{Pe}\frac{\partial \hat{T}}{\partial \bar{z}} + b_1^2\frac{\partial^2 \hat{T}}{\partial \bar{x}^2} + b_2^2\frac{\partial^2 \hat{T}}{\partial \bar{y}^2} + B\hat{T} + N_{Pe} \tag{24}$$

This differential equation can be solved with constant wall boundary conditions similar to those in the previous problem and with some initial temperature distribution by application of the principle of superposition and the Fourier method. The solution is the sum of a time-independent nonhomogeneous problem and a time-dependent completely homogeneous problem. The time-dependent portion of the solution with zero wall temperature is satisfied by an infinite series of

$$A_{nmm} \exp\left(N_{Pe}\frac{\bar{z}}{2}\right) \sin n\pi\bar{z} \cos\left(\frac{2m+1}{2}\right)\pi\bar{y} \cos\left(\frac{2m+1}{2}\right)\pi\bar{x} \exp\left[B - \left(\frac{1}{2}N_{Pe}\right)^2 - n^2\pi^2 - \left(\frac{b_2}{2}\right)^2(2m+1)^2\pi^2 - \left(\frac{b_1}{2}\right)^2(2m+1)^2\pi^2\right]\theta$$

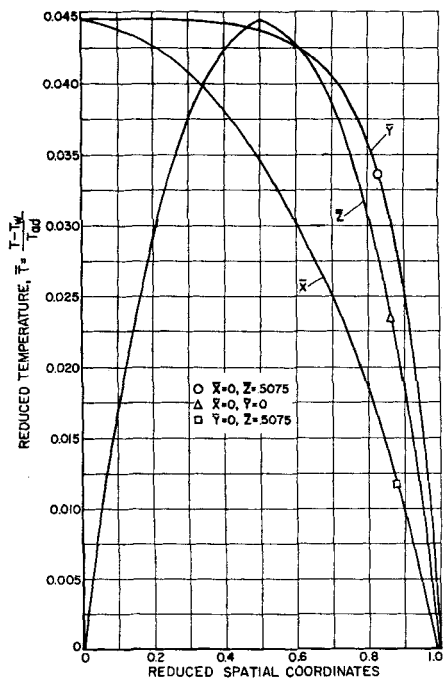

Fig. 6. Reduced temperature for a reduced inlet temperature of zero, Peclet number of 0.6, b_1 equal to 2.0, and b_2 equal to 0.5.

with n and m going from 1 and 0, respectively. Examination of the time-dependent expression shows that unless

$$\left(\frac{1}{2}N_{Pe}\right)^2 + n^2\pi^2 + \left(\frac{b_2}{2}\right)^2 (2m+1)^2\pi^2 + \left(\frac{b_1}{2}\right)^2 (2m+1)^2\pi^2 > B \quad (25)$$

the temperature will rise with time indefinitely. The process is then unstable. It is also clear that if the process is stable for the lowest eigenvalue, it is stable for all higher eigenvalues. Therefore, the critical size of the fuel cell pack satisfies the equation

$$B = \left(\frac{1}{2}N_{Pe}\right)^2 + \pi^2 + \left(\frac{b_2}{2}\right)^2\pi^2 + \left(\frac{b_1}{2}\right)^2\pi^2 \quad (26)$$

Thus, in terms of original variables for thermal stability, the expression

$$\frac{1}{(2a_1)^2} + \left(\frac{k_r}{k}\right)\frac{1}{(2a_2)^2} + \frac{1}{a_3^2} \geq \frac{\psi_1}{k\pi^2} - \left(\frac{Gc_p}{2k\pi}\right)^2 \quad (27)$$

must be true. In a fuel cell pack of larger dimensions the phenomenon of thermal buckling may take place; that is, somewhere the temperature will exceed the permissible operating temperature and cause failure. Consumption of reactants or termination of chemical reaction will prevent the rise of temperature to infinity but may not prevent the creation of hot spots causing structural failure. Thus, for safe operation, the pack dimensions must satisfy Equation (27) for a given flow rate. A square pack of linear dimension of several feet may exceed the critical dimensions with a reasonable rise of reaction rate with temperature.

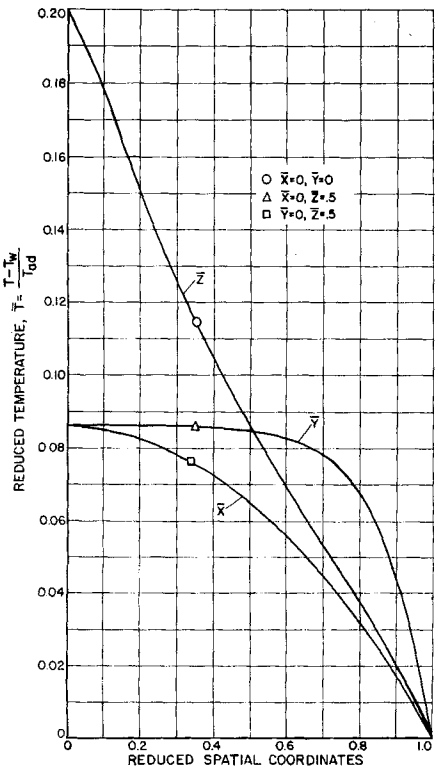

Fig. 7. Reduced temperature for a reduced inlet temperature of 0.2, Peclet number of 0.4, b_1 equal to 2.0, and b_2 equal to 0.5.

ACKNOWLEDGMENT

The investigation was supported through the basic research program of the Institute of Gas Technology. Some of the calculations and the verification of the solution to the partial differential equation were done by S. Chuck as a part of the IGT work-study program. The Fortran program was written by W. Toczycki.

Experimental data were derived from programs supported by Con-Gas Service Corporation, Southern California Gas Company, Southern Counties Gas Company of California, and the American Gas Association.

NOTATION

A = cross-sectional area, sq. ft.

a_1, a_2, a_3 = half-width, half-length, and height of the fuel cell pack (Figure 3), ft.

$B = \dfrac{\psi_1 a_3^2}{k}$, dimensionless

$b_1 = \dfrac{a_3}{a_1}$, dimensionless

$b_2 = \left(\dfrac{a_3^2 k_r}{a_2^2 k}\right)^{3/2}$, dimensionless

C = molar density of gases, lb.-moles/cu. ft.

c_p = heat capacity of gases at constant pressure, B.t.u./lb.-°F.

c_{pa} = heat capacity of the fuel cell pack, B.t.u./lb.-°F.

E = emf of the cell

F = Faraday constant, 12,158 amp.-hr./lb. equivalent

G = mass flow rate per unit of total area (superficial mass flow rate), lb./hr.-sq. ft.

H_h = height of a heat transfer unit, ft. $= \dfrac{\rho v \alpha_1 c_p}{h}$

H_m = height of a reaction rate unit, ft. $= \dfrac{\rho v \alpha_1}{K M_{av}}$

h = heat transfer coefficient on the air side of the electrode, B.t.u./hr.-sq. ft.-°F.

h' = heat transfer coefficient on the fuel side of the electrode, B.t.u./hr.-sq. ft.-°F.

I = current density, amp./sq. ft.

K = first-order reaction rate constant, defined by Equation (1), lb. moles/hr.-sq. ft.

k = effective thermal conductivity of the fuel cell battery in the direction of flow, B.t.u./hr.-ft.-°F.

k_r = effective thermal conductivity in the direction perpendicular to cells, B.t.u./hr.-ft.-°F.

L = length of fuel cell, ft.

M_{av} = average molecular weight, lb./lb. mole

m = heat transfer coefficient ratio of fuel to air $= \dfrac{h'}{h}$, dimensionless

N_{Pe} = Peclet number $= \dfrac{Gc_p a_3}{k}$, dimensionless

n = heat content ratio of fuel to air $= \dfrac{\rho' v' \alpha_3 c_p'}{\rho v \alpha_1 c_p}$, dimensionless, also number of equivalents per mole when occurring as nF.

q = heat flux per unit area, B.t.u./hr.-sq. ft.

R = electrical resistance, ohm

S = entropy, B.t.u./lb. mole-°R.

T = temperature, °F.

$\bar{T}$ = reduced temperature $= \dfrac{T - T_w}{T_{ad}}$

$\hat{T}$ = dimensionless temperature $= \dfrac{T}{T_{ad}}$

T_K = $\dfrac{3.413\,K\,(nFy_i^{\circ})^2}{2M_{av}c_p}\left(\beta_1+\dfrac{\alpha_2}{\sigma}\right)$, °F.

T_s = $\dfrac{y_i''T_m(-\Delta S)}{M_{av}c_p}+\dfrac{3.413\,nFy_i^{\circ}\beta_o}{M_{av}c_p}$, °F.

T_{ad} = an adiabatic reaction temperature = $\dfrac{\psi a_3}{Gc_p}$ or $\dfrac{\psi_o a_3}{Gc_p}$ for rate varying with temperature, °F.

T_m = average absolute temperature of the electrolyte, °R.

T_A = inlet pack air temperature, °F.

T_w = wall temperature, °F.

t = temperature of the air stream, °F.

t' = temperature of the fuel stream, °F.

t_o = inlet temperature of the air stream, °F.

t_o' = inlet temperature of the fuel stream, °F.

v = linear velocity, ft./hr.

x,y,z = length coordinates, ft.

$\bar{x},\bar{y},\bar{z}$ = $\dfrac{x}{a_1},\dfrac{y}{a_2},\dfrac{z}{a_3}$, respectively

y_i = mole fraction of the controlling species

y_i° = mole fraction of the controlling species entering the fuel cell

y_i' = mole fraction of the controlling species leaving the fuel cell

Greek Letters

α_1 = width of the air channel (Figure 1), ft.

α_2 = thickness of the electrode-electrolyte assembly (Figure 1), ft.

α_3 = width of the fuel channel (Figure 1), ft.

β_0 = intercept of linearized polarization curve in Equation (5), volts

β_1 = slope of linearized polarization curve in Equation (5), ohm-sq. ft.

θ = dimensionless time = $\dfrac{k\tau}{\rho_{pa}c_{pa}a_3^2}$

ρ = density of gas, lb./cu. ft.

ρ_{pa} = density of pack, lb./cu. ft.

σ = electrical conductivity of the electrolyte-electrode assembly, mho/ft.

τ = time, hr.

ψ = rate of heat generation per unit volume of pack, B.t.u./hr.-cu. ft.

ψ_o = intercept of the rate of heat dissipation per unit total volume vs. temperature curve defined by Equation (23), B.t.u./hr.-cu. ft.

ψ_1 = slope of the rate of heat dissipation per unit total volume vs. temperature curve, defined by Equation (23), B.t.u./hr.-cu. ft.-°F.

LITERATURE CITED

1. Austin, L. G., P. Palasi, and R. R. Klimpel, paper presented at 145th Natl. ACS Div. Fuel Chem., **1**, No. 4 (September, 8-13, 1963).
2. Carslaw, H. S., and J. C. Jaeger, "Conduction of Heat in Solids," Oxford Univ. Press, London, England (1959).
3. Eisenberg, M., in "Advances in Electrochemistry and Electrochemical Engineering," C. Tobias, Ed., Vol. 2, Interscience, New York (1962).
4. ———, and B. Baker, *Electrochem. Technol.*, **2**, 258-261 (1964).
5. Frank-Kamenetskii, D. A., "Diffusion and Heat Exchange in Chemical Kinetics," translated from the Russian edition by N. Thon, Princeton Univ. Press, Princeton, New Jersey (1955).
6. Levich, V. G., "Physicochemical Hydrodynamics," Prentice Hall, New York (1963).
7. von Fredersdorff, C. G., in "Fuel Cells," Vol. 2, Reinhold, New York (1963).

Manuscript received November 11, 1964; revision received March 24, 1965; paper accepted March 26, 1965. Paper presented at A.I.Ch.E. Los Angeles meeting.

Scale-Up for Viscoelastic Fluids

JOHN C. SLATTERY

Northwestern University, Evanston, Illinois

A suggestion is made as to how one might proceed to scale up a process involving an arbitrary viscoelastic fluid. The discussion is based upon Noll's theory of simple fluids. Turbulent flow in an infinitely long pipe is used as an illustration.

Many commercial processes involve viscoelastic* fluids from polymers and polymer solutions to food products. The behavior of these fluids is generally so complex that an accurate theoretical description of the flow in a given geometry may be out of the question. When the design engineer is faced with such a situation, one answer might be a model study, the results of which are correlated by dimensional analysis.

The most useful correlation of experimental data would be one valid for all fluids. This would permit the prediction of the results for one fluid in a given geometry on the basis of previous experiments with perhaps another fluid in a geometrically similar situation. Upon reflection, one realizes that to be able to do this it would be necessary to have a specific form of constitutive equation (an equation by means of which stress can be predicted from a knowledge of deformation) that would be valid for all fluids. Though many specific constitutive equations have been proposed, as yet none have been shown to be valid for more than a few fluids over a limited range of stress.

The next most useful scheme would allow one to predict the behavior of the fluid in the full-scale apparatus on the basis of data for the same fluid in a geometrically similar model. In what follows such an approach is out-

* Viscoelastic is used in the sense that the materials obey neither of the classical linear relations: Newton's law of viscosity and Hooke's law of elasticity.